

The contribution of DInSAR techniques for slow-moving landslide characterization



Leonardo Cascini, Settimio Ferlisi & Dario Peduto

Department of Civil Engineering – University of Salerno, Fisciano, Salerno, Italy.

Gianfranco Fornaro

Institute for Electromagnetic Sensing of the Environment (IREA-CNR), Naples, Italy.

ABSTRACT

This work shows the potential of innovative procedures for the slow-moving landslide characterization at different scales. Particularly, the procedures are based on the joint use of data obtained via Differential SAR Interferometry (DInSAR) remote sensing techniques, at both full- and low-resolution, the kinematic of the landslides and the landslide-induced damage to structures/infrastructures.

RÉSUMÉ

L'article montre le potentiel d'innovant procédures – basées sur l'usage combiné des données obtenus par les techniques d'Interférométrie Différentiel SAR (DInSAR), à les deux haute et bas résolution, avec l'aide de considérations sur la géométrie d'acquisition des détecteurs, la cinématique des glissements de terrain et les dommages expérimentés dans les structures/infrastructures qu'interagit avec les phénomènes – en caractériser les glissements de terrain à cinématique lente en ce qui concerne d'échelles d'analyse différentes.

1 INTRODUCTION

The exploitation of DInSAR data for the analysis of ground deformations related to slow-moving landslides has been tested in the scientific literature with reference to different case studies (Fruneau et al. 1996; Hilley et al. 2004; Cotecchia, 2006; Farina et al. 2006; Wasowski et al. 2008). These latter highlighted current limitations due to the complexity of instability phenomena, the sensor acquisition geometry and the availability /interpretation of DInSAR data on slopes (Colesanti and Wasowski, 2006; Cascini et al. 2010). As a consequence, the use of these data within the landslide characterization process is not yet straightforward.

To this end, the present work introduces a new methodology for DInSAR data interpretation in areas for which a proper geomorphological and topographic knowledge is available. The first step is the generation of the a priori DInSAR landslide visibility map (described in details in Cascini et al. 2009). Then, DInSAR data interpretation is based on the joint use of remote sensed data and simplified geomorphological models.

The proposed procedure is tested at both medium (1:25,000) and large (1:5,000) scales (Fell et al. 2008), within a sample area extending for around 500 km² in the territory of the National Basin Authority of Liri-Garigliano and Volturno (NBA-LGV) rivers (central-southern Italy) (Fig.1).

2 THE TEST AREA AND THE USED DATASET

Thirty-three images (track 308 - frame 2765), acquired over descending orbits of the ERS1-ERS2 satellite systems (period March 1995 - February 2000), have been processed via the Enhanced Spatial Differences (ESD) approach (Fornaro et al. 2009a,b), which

represents an upgrading of the original SBAS algorithm (Berardino et al. 2002). This algorithms allow the generation of both low-resolution DInSAR maps (with pixel on the ground of approximately 80 x 80 m) and full-resolution maps (with pixel on the ground of approximately 10 x 10 m).



Figure 1. The test area.

For the test area both base and thematic maps are available at 1:25,000 scale. The maps were produced in 2001 as results of the activities of the PSAI project (Piano Stralcio per l'Assetto Idrogeologico), carried out by a group of experts and technicians working for NBA-LGV. The activity was developed in accordance with the Act of Italian Parliament (L. 365/2000), aimed to zone both landslide hazard and risk all over the Italian territory (Cascini, 2008). Referring to base maps, the geological map highlights that the bedrock mainly consists of Upper Miocene arenaceous units mantled by Quaternary Age

superficial deposits, characterized by talus and alluvial fans. The Landslide inventory map, derived from aerial photographs and surface surveys, indicates that the phenomena cover around 5% of the whole territory. This last map furnishes detailed information for each mapped phenomena with reference to location, typology, state of activity and areal extension (Cascini et al. 2005).

Owing to the phase ambiguity limitation of DInSAR data processing (for more details refer to Cascini et al. 2010), the analysis of landslides focuses on the typology of phenomena ranging from extremely to very slow velocity classes (i.e. lower than 1,6 m/year according to Cruden and Varnes, 1996). In the study area a total number of 897 slow-moving landslides are mapped (Peduto, 2008; Cascini et al. 2009). According to Varnes (1978) they are classified as: 204 rotational slides, 238 earth flows, 78 rotational slides-earth flows, 336 creeps, 33 earth flows - creeps, 8 deep-seated gravitational movements. On the basis of geomorphological criteria, three different states of activity are distinguished for these landslides, defined as follows: “active” (including active, reactivated and suspended), “dormant” and “inactive” (relict) phenomena (Cruden and Varnes, 1996). The selected landslide typologies exhibit a significant predominance of dormant phenomena (428) on active ones (92). This is confirmed by the available dataset on damage to buildings and roads interacting with the displaced masses, showing that damage was recorded to 30% of the surveyed buildings and 24% of the investigated roads (Cascini et al. 2008).

3 THE PROCEDURE PROPOSED FOR DINSAR APPLICABILITY TO LANDSLIDES

The framework sketched in Figure 2 describes the procedure developed for DInSAR data analysis at different scales.

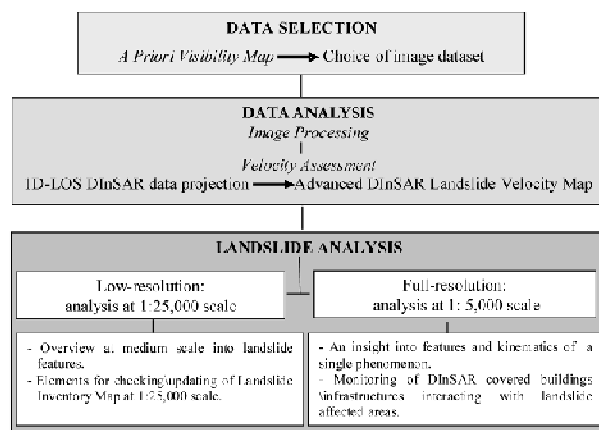


Figure 2. The framework of DInSAR data analyses for landslide studies (from Cascini et al. 2010).

The first step consists of the generation of the a priori DInSAR landslide visibility map (Peduto, 2008; Cascini et al. 2009), which can be used to distinguish in advance whether an area is expected to be visible from space-borne SAR sensors thus driving data-users through the image dataset selection.

Once SAR images have been processed, if an adequate knowledge of landslide phenomena is available, a procedure for 1D-LOS DInSAR data projection can be implemented to generate the advanced DInSAR landslide velocity map.

As for the scale of the study, low-resolution DInSAR data can be used for landslide analyses at 1:25,000 scale, according to the dimension of both the landslide phenomena and the coherent DInSAR pixels on the ground. Full-resolution DInSAR data allow studies at more detailed scale (i.e. 1:5,000) according to the almost point-wise information and the dimension of single portions of landslides and structures/ infrastructures.

3.1 A priori visibility map

The choice of the most suitable SAR image dataset represents a key step for DInSAR data exploitation in landslide studies, since the visibility of a certain portion of a slope depends on several factors such as slope aspect and inclination, vegetation cover, presence of buildings/infrastructures. The role played by the aspect angle and the slope inclination, which have a direct impact on the feasibility of DInSAR deformation monitoring, has been already discussed in Colesanti and Wasowski (2006), Peduto (2008), Cascini et al. (2009).

Following the procedure described in details in Peduto (2008) and Cascini et al. (2009), here an example of the a-priori DInSAR landslide visibility map over a portion of the study area, obtained via low-resolution ESD DInSAR data, is presented at 1:25,000 scale (Fig. 3). The input data consist of the following available maps: landslide inventory map; aspect map; slope angle map; land-use map; urbanised area map. Particularly, by intersecting the aspect map and the slope angle map *visible/ visible with difficulty/ not visible areas* are zoned.

By merging the land-use map and the urbanised area map, vegetated areas are removed from those portions classified as visible according to geometric considerations, thus obtaining the so called “a priori DInSAR landslide visibility map”. The validation of the map for the whole test area (partially shown in Figure 3) proves that 67% out of a total of 215 low-resolution DInSAR coherent pixels intersecting landslide affected areas concentrate on *visible areas*; 19% lay on areas visible with difficulty; only 14% can be found in areas assumed as *not visible*. The described procedure can be easily applied at 1:5,000 scale if base and derived maps are available at this scale.

3.2 1D LOS DInSAR data projection and the generation of the advanced DInSAR landslide velocity map

The procedure for the projection of 1D LOS DInSAR velocity vectors, based on both geomorphological and DEM models, is described in Peduto (2008) and Cascini et al. (2010). The flow-chart for the generation of the advanced DInSAR landslide velocity map is shown in Figure 4.

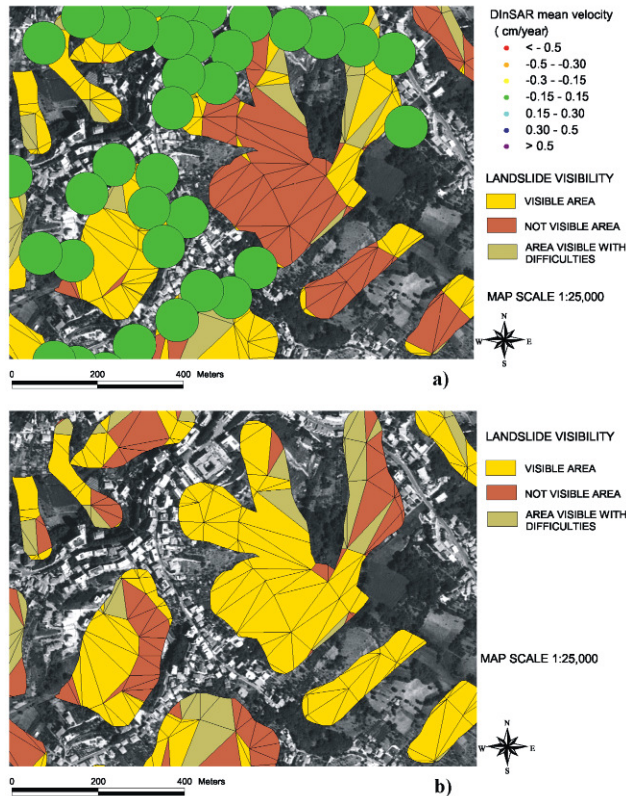


Figure 3. The “a priori DInSAR landslide visibility map”: (a) on descending orbits with low-resolution DInSAR coherent pixel distribution; (b) on ascending orbits (from Cascini et al. 2009).

On this map DInSAR coherent pixels are represented depending on several factors to be taken into account. Particularly, conditions of movement/no-movement depend on whether the mean velocity of the DInSAR coherent pixel exceeds the fixed velocity threshold. Moreover, the direction of movement is assumed consistent with the geomorphological scheme of the landslide on which each DInSAR coherent pixel is located. Finally, the projected velocity value is assumed as a reliable value if the condition number does not exceed the fixed threshold (Cascini et al. 2010).

4 LOW-RESOLUTION LANDSLIDE ANALYSIS

According to the scheme in Figure 4, the advanced low-resolution DInSAR landslide velocity map was developed at 1:25,000 scale, for all the test area in NBA-LGV, to analyze rotational slides, earth flows and rotational slides-earth flows, whose total amount is 553; 185 (around 33%) of those resulted covered by DInSAR data.

The map highlights that almost 84% of the DInSAR covered dormant landslides (144) exhibit evidence of no-movement. On the other hand, the percentage of active landslides (25) with moving coherent DInSAR pixels is about 24%, on the average (Cascini et al. 2008). An example is reported with reference to the municipalities of Frosinone and Torrice (Lazio region) in Figure 5, where very few moving low-resolution DInSAR pixel are detected over an area of about 3 km x 6 km essentially including dormant phenomena.

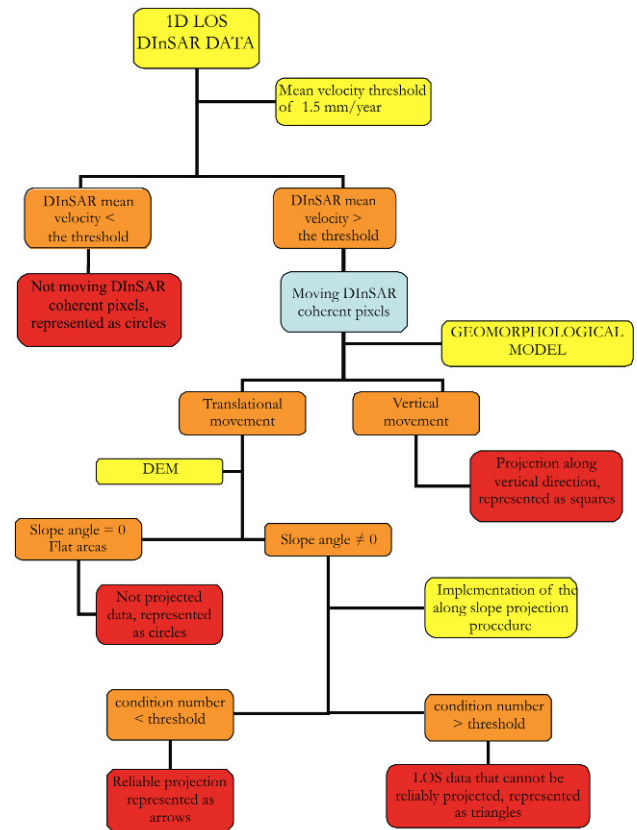


Figure 4. Flow-chart for the generation of the advanced DInSAR landslide velocity map (from Cascini et al. 2010).

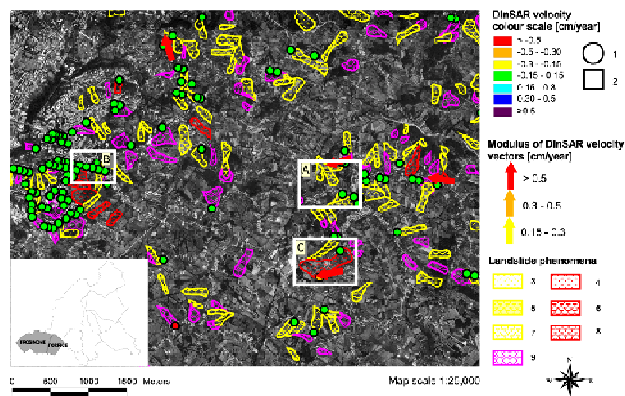


Figure 5. An example of advanced low-resolution DInSAR landslide velocity map for the municipality of Frosinone and Torrice (Lazio Region, Italy). 1) Not moving DInSAR coherent pixel or on flat areas; 2) DInSAR coherent pixel moving on vertical direction; 3) dormant rotational slide; 4) active rotational slide; 5) dormant earth flow; 6) active earth flow; 7) dormant rotational slide – earth flow; 8) active rotational slide – earth flow; 9) creep phenomenon (from Cascini et al. 2010).

Within this area, the directions of movement (see the four red arrows), derived by modelling the available 1D LOS DInSAR data, seem congruent with the assumption of the geomorphological schemes (downward direction along slope). Moreover, the highest projected mean velocities are attained in the main body, independently of the landslide typology (Fig. 6).

The advanced low-resolution map were then used to detect new landslide phenomena within the test area by extending the analysis of moving/not moving coherent pixels on those portions of the territory mapped as hollows in the geomorphological map at 1:25,000 scale (Cascini et al. 2009). These zones (1,263 in the investigated area) are characterized by geomorphological settings quite similar to landslide-affected areas, also exhibiting the same landslide predisposing factors. Indeed, as for 63 hollows a clear evidence of movement was recorded; this can provide elements for a check/update of the landslide inventory map that represents the starting point for the landslide risk analysis as described in Fell et al. (2008).

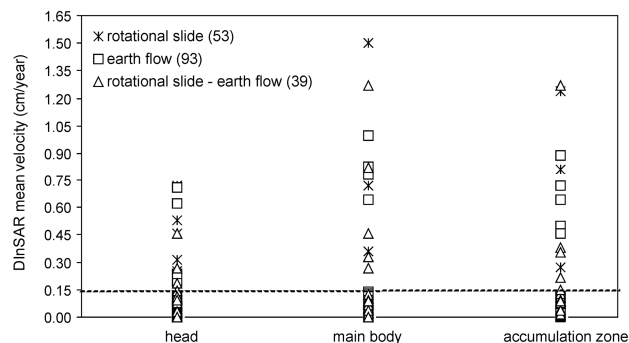


Figure 6. DInSAR mean velocities recorded within covered landslides: 53 rotational slides; 93 earth flows; 39 rotational slides – earth flows (from Cascini et al. 2010).

5 FULL-RESOLUTION LANDSLIDE ANALYSIS

Analyses of landslide phenomena at more detailed scale (i.e. 1:5,000) can exploit full-resolution DInSAR data following the flow-chart in Figure 4. However, since these analyses call for significant computational efforts, they can be concentrated on limited areas. Taking this in mind, two main goals were pursued: the preliminary analysis of landslide features (i.e. check of mapped boundaries; detection of ground displacement out of mapped areas); getting an insight into different kinematic behaviour characterizing different portions of the same phenomenon.

5.1 Analysis of landslide features

In order to check possible changes in landslide boundaries, the entire full-resolution coherent pixel dataset was projected assuming translational movements along the steepest slope direction for the pixels out of the mapped landslides. Some examples on this are reported in Cascini et al. (2010); here, a portion of the municipality of Frosinone (Fig. 7), highlighting evidence of movements both inside and outside the landslide boundaries, is shown. Particularly, special attention is worth being paid to full-resolution DInSAR coherent pixels exhibiting mean velocity values exceeding 0.3 cm/year within two dormant earth flows (labelled with letters A and D) and creep zones (labelled with letters B and C) as well as the areas framed with the circle and the square, respectively. As for the zone framed with the circle, a cross check via the geomorphological map shows that the buildings in the area were built on an hollow showing evidences of movement for the period 1995-2000, on the basis of DInSAR data.

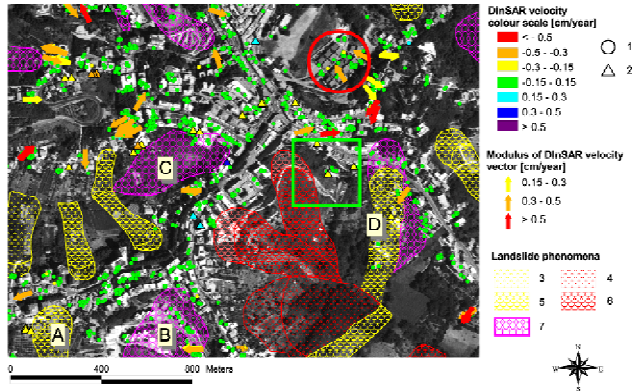


Figure 7. Overview of Advanced full-resolution DInSAR landslide velocity map for a portion of the municipality of Frosinone (Lazio Region, Italy). 1) Not moving DInSAR coherent pixel or on flat areas; 2) not projected translational displacement owing to high condition number; 3) dormant rotational slide; 4) active rotational slide; 5) dormant earth flow; 6) active earth flow; 7) creep phenomenon (Cascini et al. 2010).

The area framed by a rectangle highlights the presence of moving full-resolution DInSAR coherent pixels in proximity of a landslide classified as active earth flow in the landslide inventory map at 1:25,000 scale.

In this case further analyses carried out via a map at 1:5,000 scale of the landslide affected areas (Cascini et al. 2010) allow to point out that the moving coherent pixels fall within a small active rotational slide – earth flow; on the contrary, the stable coherent pixels are located within the head of the dormant rotational slide – earth flow. This stresses that the reliability of full-resolution DInSAR data must be necessarily checked via thematic and topographic maps at 1:5,000 scale.

5.2 The case study of La Consolazione landslide

“La Consolazione” landslide is a rotational slide – earth flow, located within Torrice municipality (Lazio region, Italy), which twice reactivated in the last decades (1986; 1990). The landslide, having an areal extension of around 12 ha, exhibits the typical shape of a rotational slide – earth flow with a width ranging from 100 ÷ 150 m (in the head where the rotational mechanism develops) up to 250 m (in the accumulation zone where the enlarging earth flow prevails). Furthermore, in the upper accumulation zone (between the elevations of 200 and 220 m a.s.l.) evidence of creep phenomena (e.g. ripples on the ground surface) can be distinguished.

The available documents report that in 1986 only the narrow upper portion (Fig. 8a) reactivated; then, in the 90s subsequent reactivations involved the portion of the landslide that stretches from the creeping zone down to the toe.

On the basis of the above information and aerial photographs, an updated map of the landslide was produced at 1:5,000 scale showing three main portions: the old main scarp and the old terraced accumulation

zone with evidence of cracks; the recent minor scarp (215 m a.s.l.) bordering the reactivated earth flow; the old accumulation zone. Referring to the state of activity, the upper portion of the landslide, as well as the old accumulation zone were mapped as dormant; whereas the remaining portion corresponds to the reactivated earth flow.

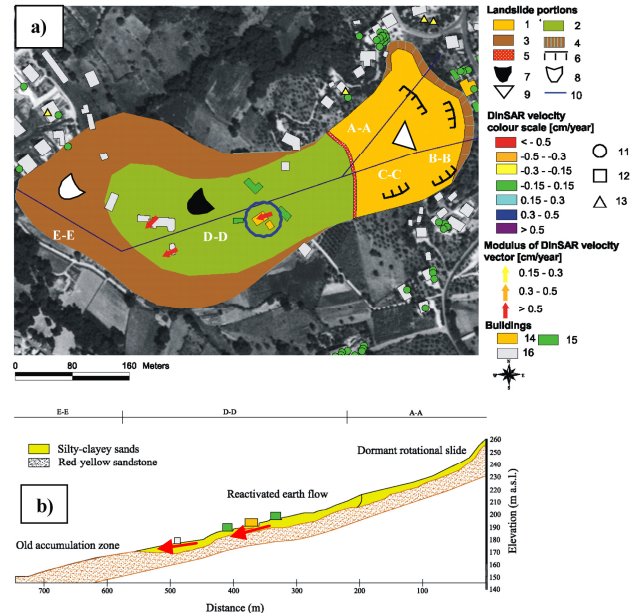


Figure 8. La Consolazione landslide (Lazio region, Italy): a) Map of the landslide with buildings and Advanced full-resolution DInSAR velocity data; b) Longitudinal cross section of the landslide with buildings and DInSAR velocity vectors: 1)terraced old accumulation zone; 2)reactivated old accumulation zone; 3) old accumulation zone; 4) old scarp; 5) recent scarp; 6)cracks; 7)reactivated earth flow; 8) dormant earth flow; 9) dormant rotational slide; 10) cross-section; 11) not moving DInSAR coherent pixel or moving coherent pixel on flat areas; 12) DInSar coherent pixel moving on vertical direction; 13) not projected translational displacement owing to high condition number; 14) damaged building; 15) building without damage survey; 16)building without damage survey (from Cascini et al. 2010).

Figures 8a and 8b show, respectively, a map and a cross-section of the advanced full-resolution DInSAR velocity map superimposed to both the building map and the landslide map at 1:5,000 scale.

The analysis of the mean velocity values for the 1995-2000 period highlights that the full-resolution coherent pixels located near the old scarp exhibit no evidence of movement; those located within the reactivated portion are moving with mean velocity values higher than 0.5 cm/year (Figures 8a and 8b). This is in agreement with the updated map of the landslide at 1:5,000 scale and information deriving from the DInSAR covered buildings in the area that shows the evidence of

movement recorded to two buildings (framed with the circle in Figure 8a and located in the central portion of the reactivated landslide) matching the damage occurrence as observed by the damage survey.

6 CONCLUSIONS

In the last decade the use of remote sensing data derived from DInSAR techniques has rapidly grown thanks to the development of enhanced image processing algorithms and their increased availability that, as in the case of the Italian territory, can reach the total coverage.

Consequently, there is the need of a confident use of these data to overcome some problems still arising in the analysis of slow-moving landslides. In this regard, this research introduces an innovative procedure that allows a significant improvement of the common 1D DInSAR velocity maps at both low- and full-resolution. These maps – as a result of considerations on sensor acquisition geometry, topography and landslide features – can provide valuable enhancements to DInSAR data use for landslide characterization. In this regard, the example shown for the test area proved the possibility of checking the boundaries and the state of activity of mapped landslides, the detection of possible unmapped phenomena as well as the monitoring of facilities interacting with them.

The results obtained seem particularly appealing considering the enhanced capabilities of the newest sensor (e.g. TerraSAR_X, COSMO/SKYMED, etc) which will offer high resolution DEMs, three times higher data acquisition frequency, and an increase in the sensitivity to temporal decorrelation via the reduction of the wavelength.

References

- Berardino, P., Fornaro, G., Lanari R. and Sansosti, E. 2002. A New Algorithm for Surface Deformation Monitoring based on Small Baseline Differential SAR Interferograms. *IEEE Trans. Geoscience and Remote Sensing*, 40(11): 2375-2383.
- Cascini L. 2008. Applicability of landslide susceptibility and hazard zoning at different scales. *Engineering Geology*. 102(3-4): 164-177.
- Cascini, L., Bonnard, Ch., Corominas, J., Jibson, R. and Montero-Olarte, J. 2005. Landslide hazard and risk zoning for urban planning and development. State of the Art Report (SOA7). Proceedings of the International Conference on "Landslide Risk Management", Vancouver (Canada). O. Hungr, R. Fell, R. Couture and E. Eberthardt (eds.). Taylor and Francis, London: 199-235.
- Cascini, L., Fornaro, G. and Peduto, D. 2010. Advanced low- and full-resolution DInSAR map generation for slow-moving landslide analysis at different scales. *Engineering Geology*, 112(1-4): 29-42,
- Cascini, L., Fornaro, G. and Peduto, D. 2009. Analysis at medium scale of low-resolution DInSAR data in slow-moving landslide-affected areas. *ISPRS Journal of Photogrammetry and Remote Sensing*, 64(6): 598-611.
- Cascini, L., Ferlisi, S., Peduto, D., Pisciotta, G., Di Nocera, S. and Fornaro G. 2008. Multitemporal DInSAR data and damages to facilities as indicators for the activity of slow-moving landslides. In: *Landslides and Engineered Slopes. From the Past to the Future*. Chen Z., Zhang J., Li Z., Wu F., Ho K. (eds.). Proceeding of the 10th International Symposium on Landslides and Engineered Slopes, Xi'an (China), Taylor and Francis Group, London. Vol. 2: 1103-1109.
- Colesanti, C. and Wasowski, J. 2006. Investigating landslides with space-borne Synthetic Aperture Radar (SAR) interferometry. *Engineering Geology*, 88, 173-199.
- Cotecchia, V. 2006. The Second Hans Cloos Lecture. Experience drawn from the great Ancona landslide of 1982. *Bull. Eng. Geol. Env.*, 65: 1-41.
- Cruden, D.M. and Varnes D.J. 1996. Landslide types and processes. In: Turner, A.K. and Schuster, R.L. (eds.) *Landslides, Investigation and Mitigation, Transportation Research Board Special Report 247*, Washington D.C.: 36-75.
- Farina, P., Colombo, D., Fumagalli, A., Marks, F. and Moretti S. 2006. Permanent Scatterers for landslide investigations: outcomes from the ESA-SLAM project. *Engineering Geology*, 88: 200-217.
- Fell, R., Corominas, J., Bonnard, Ch., Cascini, L., Leroi E. and Savage, W.Z. 2008. Guidelines for landslide susceptibility, hazard and risk zoning for land-use planning. *Engineering Geology*, 102(3-4): 99-111.
- Fornaro, G., Pauciuolo, A. and Serafino, F. 2009a. Deformation monitoring over large areas with multipass differential SAR interferometry: A new approach based on the use of spatial differences. *International Journal of Remote Sensing*, 30 (6): 1455-1478.
- Fornaro, G., Reale, D. and Serafino, F. 2009b. Four-Dimensional SAR Imaging for Height Estimation and Monitoring of Single and Double Scatterers", *IEEE Trans. Geosci. Remote Sens.*, 47 (1), 224-237.
- Fruneau, B., Achache, J. and Delacourt, C. 1996. Observation and Modeling of the Saint-Etienne-de-Tinée Landslide Using SAR Interferometry. *Tectonophysics*, 265: 181-190.
- Hilley, G.E., Burgbman, R., Ferretti, A., Novali, F. and Rocca F. 2004. Dynamics of slow-moving landslides from Permanent Scatterer Analysis. *Science*, 304: 1952-1955.
- Peduto, D. 2008. *Analysis of ground deformations related to subsidence and landslide phenomena via DInSAR techniques*. Ph.D. Thesis (In English). University of Salerno, Italy. Tutor: Cascini L.; co-tutor: Fornaro G.
- Varnes, D.J. 1978 Slope movements. Types and processes. In: *Landslides: analysis and control*, (Schuster R.L. & Krizker R.J. Eds.) Nat. Acad. of

Sciences, Transp. Res. Board, Washington, 1978.
Special Report 76:11-35.

Wasowski, J., Casarano, D., Bovenga, F., Refice, A., Nutricato, R. and Nitti, D.O. 2008. Landslide-prone towns in Daunia (Italy): PS interferometry-based investigation. In: *Landslides and Engineered Slopes. From the Past to the Future*. Chen Z., Zhang J., Li Z., Wu F., Ho K. (eds.). Proceeding of the 10th International Symposium on Landslides and Engineered Slopes, Xi'an (China), Taylor and Francis Group, London. Vol. 1: 513-518.